JOURNAL OF MATERIALS SCIENCE 17 (1982) 832–842

Prediction of failure modes in unidirectional short-fibre composites*

HARUO ISHIKAWA†, TSU-WEI CHOU, MINORU TAYA
Department of Mechanical and Aerospace Engineering, University of Delaware, Newark, Delaware 19711, USA

In short-fibre reinforced composites, penny-shaped cracks often initiate from fibre-ends and propagate into the matrix until they are arrested by the neighbouring fibres. A theoretical study on the prediction of failure modes after the arrest, that is, either the penetration of the crack into the fibres or the debonding of the matrix–fibre interface, is performed. The analytical method used in this study is the extension of the two-dimensional model of Kendall to the three-dimensional crack problem. Strain energy release rates for the initiation of the cracks of the penetration and debonding types are calculated. Also computed are the total potential energy required for a complete penetration of the crack through the fibre diameter and a complete debonding of the matrix–fibre interface. Based on these computations, the failure modes of the crack arrested by the neighbouring fibres are discussed.

1. Introduction

It has been reported [1, 2] that in a short-fibre reinforced composite microcracks can initiate at fibre-ends at a strain level lower than the failure strain of the pure matrix material and propagate into the matrix under increasing applied load until they are arrested by the neighbouring fibres. The cracks so initiated seem to grow as penny-shaped cracks with their crack planes perpendicular to the applied load. The stiffness and strength of aligned short-fibre reinforced composites containing fibre-end cracks, before they are arrested by the neighbouring fibres, have recently been investigated by Taya and Mura [3], and Takao *et al.* [4].

When the penny-shaped crack is arrested by the fibres at a right-angle in aligned short-fibre composites, an important question arises as to the direction of further propagation of the crack: the crack will either penetrate into the fibre along the existing crack plane or cause debonding of the matrix–fibre interface. The answer to this question is difficult, if not impossible, to obtain due to the three-dimensional problem, researchers have often focused their attention on the crack-tip stress singularity. The works of Bogy [5] and Comninou [6] are typical in this approach. However, neither the energy release rate nor the critical applied stress has been treated for the case of a crack meeting an interface. To our knowledge, under only very restricted conditions, Sanchez-Moya and Pipkin [7] computed the energy release rate of a two-dimensional crack meeting an interface at a right-angle. The assumptions they made are the incompressibility of the composite, the inextensibility of the fibre and the infinite aspect ratio of the fibre. They termed such a combination of fibre and matrix an "ideal composite". Based upon these assumptions, the energy release rate for the initiation of a crack, which would penetrate into the fibre, was obtained, but the energy required for the crack to fracture a fibre could not be estimated.

As to the problem of matrix–fibre interfacial debonding, a number of attempts (for example, [8, 9]) have been made to theoretically predict

*This research was supported by the National Science Foundation under Grant No. CME-7918249.
†On leave from Department of Mechanical Engineering, University of Electro-Communications, Tokyo, Japan.

 0022–2461/82/030832–11$03.82/0

and to experimentally measure the energy for debonding. In the work of Kelly [9], the prediction of the fracture energy for debonding of the interface, γ_I, is based on the assumption that the interface is broken by the interfacial shear stress. The value of γ_I thus obtained depends on the fibre diameter, the fracture stress and Young's modulus of the fibre. However, the experiment for determining γ_I was carried out using fibres of diameters larger than that used in the usual short-fibre reinforced composites and, thus, the measured value of γ_I may not necessarily represent those of the practical systems. It should also be noted that the criterion for interfacial debonding discussed in [8, 9] is given in such a manner that the applied stress does not play any role in affecting debonding.

Williams and Reifsnider [10] examined both theoretically and experimentally the occurrence of failure modes, including debonding, delaminations and fibre breakage, in composite materials, using the strain energy release rate method. However, their models were different from the case of debonding and fibre breakage caused by a crack meeting an interface, as examined in this paper.

Kendall [11, 12] has developed a simple two-dimensional analysis by which the behaviour of a crack meeting an interface at a right-angle can be predicted. He has also proposed several experimental methods to measure the fracture energies, γ, of a homogeneous material and the interface of a two-phase material. The value of γ so obtained agrees well with that measured by the conventional fracture mechanics type of test. The experimental method of Kendall was originally developed for a rubber-matrix composite and its applicability to other types of composites remains to be justified. Nevertheless, the model of Kendall has the merit of simplicity in calculation, and the applicability to cracks of complex geometry.

We extend Kendall's model to the three-dimensional crack problem in short-fibre reinforced composites where a penny-shaped crack originated at a fibre end and is arrested by the neighbouring fibres. Then the modes of crack propagation, namely, the penetration of the crack into a fibre and the debonding of the interface, will be discussed. Numerical calculations are performed for a graphite short-fibre reinforced epoxy. The crack model and formulation are given in Section 2, and the results and discussions are in Section 3. The conclusions will be given in Section 4.

2. Modelling and formulation

In order to simulate the situation of a crack meeting the neighbouring fibres in the composites, a simple model is constructed, as shown in Fig. 1. The infinite body contains a penny-shaped crack arrested by two neighbouring short fibres, and is subjected to the uniaxial applied stress, σ_0. The length and the diameter of the fibre are l and c_2, respectively, and the radius of the penny-shaped crack is c_1. The thickness of the crack is assumed to be infinitesimal. It is noted, in passing, that the following approach will be valid for the case of three or more neighbouring fibres. The cases of the penny-shaped crack penetrating through the fibre, and the debonding of the interface are discussed in Sections 2.1 and 2.2, respectively.

2.1. Penetration

In this section, the problem that a penny-shaped crack penetrates two neighbouring fibres is

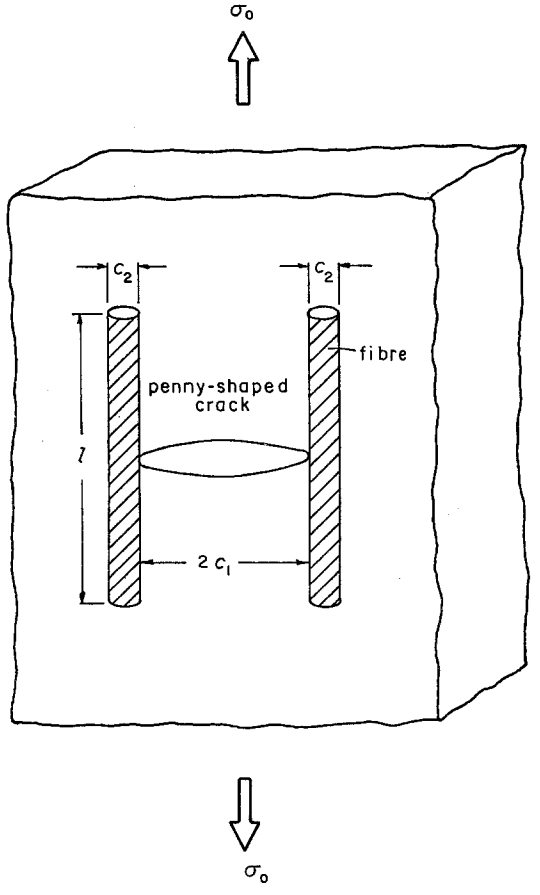

Figure 1 A penny-shaped crack arrested by two neighbouring short-fibres in an infinite body subjected to the uniaxial applied stress.

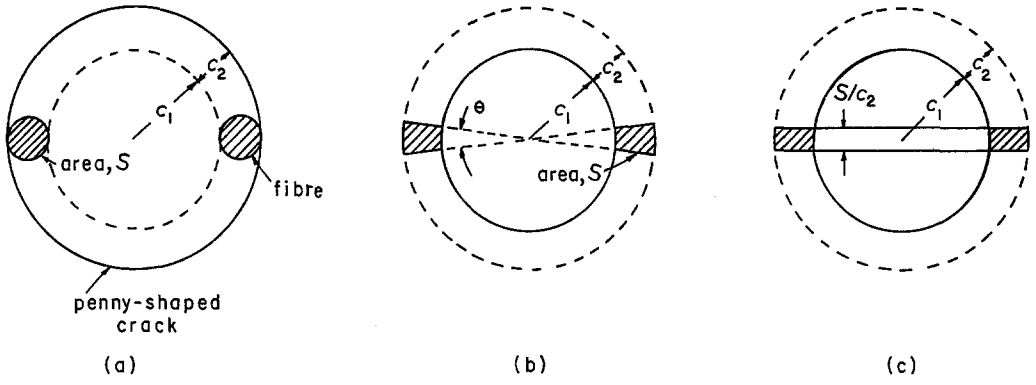

Figure 2 (a) A penny-shaped crack that has penetrated two fibres completely and has become a larger concentric crack of radius $c_1 + c_2$. (b) Conversion of the circular cross-section of the fibre to a fan-shaped section. (c) Further conversion to a rectangular section that has the same area, S, as the circular one.

modelled and, using the model, the method is formulated for obtaining the applied stress required for the crack penetration. Fig. 2a shows the cross-section of the penny-shaped crack that has penetrated two fibres completely and has become a larger crack of radius $c_1 + c_2$, concentric with the original crack. In Figs 1 and 2a the fibre at the end of which the penny-shaped crack has initiated is omitted. In order to obtain the applied stress required for the crack to penetrate the fibres, the strain energy release rate at the initiation of the penetration and the difference between the total potential energy before the penetration (Fig. 1) and that after the penetration (Fig. 2a) are considered.

In general, a fibre has a circular section. However, for convenience sake, it is assumed for the present that the fibre has a fan-shaped section. The area, S, shown in Fig. 2b, is the same as the circular section of the fibre, shown in Fig. 2a. The fan-shaped section is defined by the angle, θ, which is a function of volume fraction, V_f, of fibres. By adopting the definition of V_f given in [1], the relationship between V_f and θ is given as

$$\left[\left(\frac{\pi}{V_f}\right) + 1\right]\theta = \frac{\pi}{2}. \quad (1)$$

For example, when $V_f = 0.5$, $\theta = 0.45$ (26°), and when $V_f = 0.3$, $\theta = 0.37$ (21°). Since the angle is not very large, the fan-shaped section may be further converted to a rectangular section that also has the same sectional area, S, as shown in Fig. 2c. Finally, the plain-strain problem will be considered involving the rectangular section of fibres (Fig. 3). Fig. 3a shows that a two-dimensional crack just meets the fibres and Fig. 3b shows that the crack penetrates the fibres completely.

The difference of the total potential energy between the stage of Fig. 3a and the stage of Fig. 3b is denoted by ΔU_f for the fibre and by ΔU_m for the matrix. In case of the matrix, the opening angle shown in Fig. 2b is $2\pi - 2\theta$. Then, the difference of the total potential energy between the case that the penny-shaped crack meets the two fibres (Fig. 1) and the case that the crack penetrates the fibres completely (Fig. 2a) is given by

$$\Delta U = \Delta U_f\left(c_1 + \frac{c_2}{2}\right)(2\theta) + \Delta U_m\left(c_1 + \frac{c_2}{2}\right)(2\pi - 2\theta). \quad (2)$$

2.1.1. Initiation of penetration crack

At first, the initiation of the penetration crack will be considered, as shown in Fig. 3a. The strain energy release rate, R_{pi}, for the initiation of the penetration crack is given by Kendall [12] as

$$R_{pi} = \frac{\pi(1-\nu_m^2)c_1(c_1+c_2)^2E_f}{(c_1E_m + c_2E_f)^2}\sigma_0^2, \quad (3)$$

where E_f and E_m are the Young's moduli of the fibre and matrix, respectively, and ν_m is the matrix Poisson's ratio. Equation 3 can be modified to

$$\frac{R_{pi}}{(\sigma_0^2\pi(1-\nu_m^2)c_1)/E_m} = \frac{(1+c)^2E}{(1+cE)^2} \equiv \beta_1, \quad (4)$$

where $c = c_2/c_1$ and $E = E_f/E_m$. β_1 in Equation 4 is the non-dimensional strain energy release rate. The variation of β_1 is plotted in Fig. 4 as a function of c_2/c_1 for several values of the parameter E.

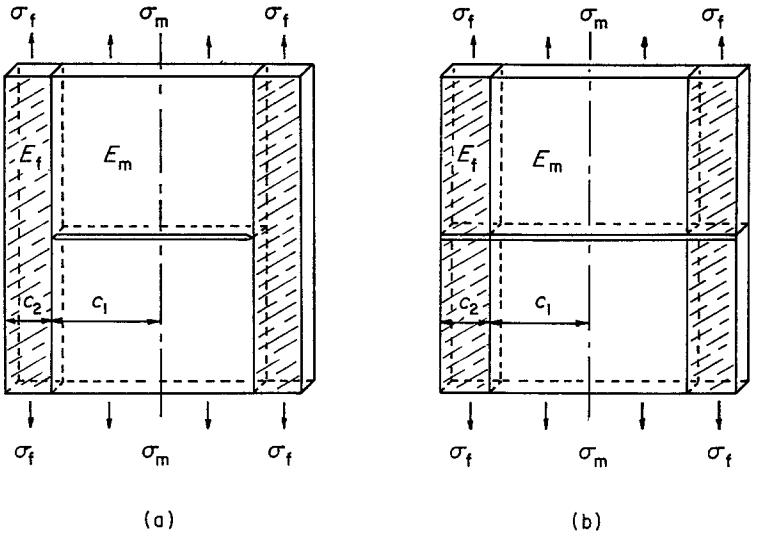

Figure 3 Plain-strain problem involving the rectangular cross-section of fibres. (a) Two-dimensional crack just touching the fibres; (b) the crack has completely penetrated into the fibres.

The strain energy release rate, R_{pi}, is also related to the surface energy of the fibre material, γ_f, as

$$R_{pi} = 2\gamma_f. \tag{5}$$

Then, using Equations 4 and 5, we can easily get the applied stress, $\sigma_0 (\equiv \sigma_{01})$ required for the initiation of the penetrating crack

$$\sigma_{01} = \left(\frac{2\gamma_f E_m}{\pi(1-\nu_m^2)c_1} \frac{1}{\beta_1} \right)^{1/2}. \tag{6}$$

It should be noted, however, that the strain energy release rate is computed for the model shown in Fig. 3a, and therefore is an approximation of the strain energy release rate for the initiation of the penetrating crack shown in Fig. 1.

2.1.2. Propagation of the penetrating crack

In order to obtain the difference in the total potential energy between for the configuration of Fig. 3a and b, the strain energy release rate for the propagation of the two-dimensional crack in the fibre region is formulated. When the crack tip is located in the fibre region, the fibre is divided into two regions, namely, cracked fibre region of width, c (c is the crack length in the fibre) and uncracked one of width $c_2 - c$.

We assume the isostrain deformation of the system under uniaxial applied load. The average Young's modulus, $\bar{E}$, and the average applied stress, $\bar{\sigma}$, of the cracked fibre region and the matrix region are

$$\bar{E} = \frac{c_1 E_m + c E_f}{c_1 + c} \tag{7}$$

and

$$\bar{\sigma} = \frac{c_1 \sigma_m + c \sigma_f}{c_1 + c}, \tag{8}$$

where σ_m and σ_f are the applied stresses in the matrix and the fibre, respectively. Thus, the problem that the crack tip is located in the fibre region can be modified to a two-phase composite problem consisting of the uncracked fibre and the cracked region that has the average Young's modulus, $\bar{E}$, and the average applied stress, $\bar{\sigma}$.

From the concept of a modified Griffith criterion by Kendall [12],

$$\sigma_f = \left(\frac{E_f R_{pp}}{\pi(1-\nu_m^2)(c_1 + c)} \right)^{1/2} \tag{9}$$

and

$$\bar{\sigma} = \left(\frac{\bar{E}^2 R_{pp}}{\pi(1-\nu_m^2)(c_1 + c)E_f} \right)^{1/2}, \tag{10}$$

where R_{pp} is the strain energy release rate. Then, the average applied stress $\sigma_0 (\equiv \sigma_{02})$ can be obtained as

$$\sigma_{02} = \frac{(c_1 + c)\bar{\sigma} + (c_2 - c)\sigma_f}{c_1 + c_2}. \tag{11}$$

Substituting Equations 9 and 10 into Equation 11, we have

$$R_{pp} = \frac{\pi(1-\nu_m^2)(c_1 + c_2)^2(c_1 + c)E_f}{(c_1 E_m + c_2 E_f)^2} \sigma_{02}^2. \tag{12}$$

The difference between the total potential energies of Fig. 3a and b can be regarded as the integration of the strain energy release rate as the crack penetrates through the fibre:

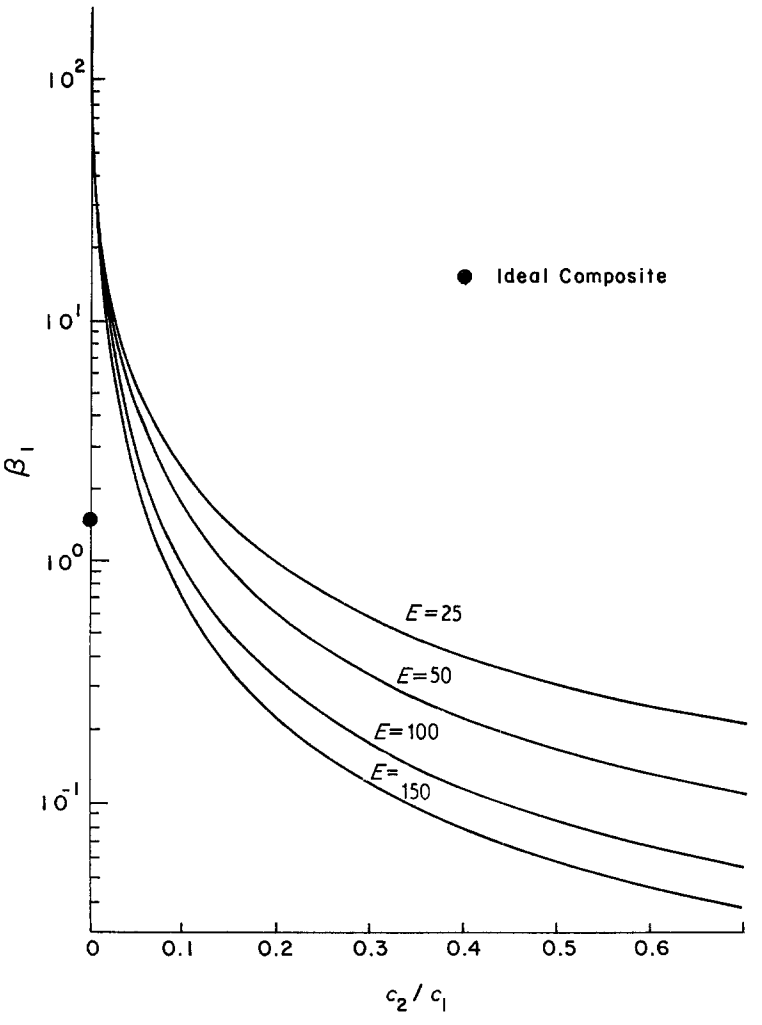

Figure 4 Non-dimensional strain energy release rate, $\beta_1 = R_{pi}/\pi(1-\nu_m^2)c_1\sigma_{01}^2/E_m$, for the initiation of a penetration crack.

$$\Delta U_f = \int_{\alpha}^{c_2} R_{pp}\, dc, \qquad (13)$$

where $\alpha \to 0$. $\alpha = 0$, namely, the initiation of the penetration crack is not included in Equation 13. Substituting Equation 12 into Equation 13, we obtain

$$\Delta U_f = \frac{\pi(1-\nu_m^2)c_1^2}{E_m}\beta_2\sigma_{02}^2, \qquad (14)$$

where

$$\beta_2 = \frac{(1+c)^2\ c+\frac{c^2}{2}\ E}{(1+cE)^2}. \qquad (15)$$

The variation of β_2 is plotted as a function of c for several values of E in Fig. 5. In the case of $E_m = E_f$, from Equations 12 and 13, the difference of the total potential energy, ΔU_m, is

$$\Delta U_m = \frac{\pi(1-\nu_m^2)c_1^2}{E_m}\beta_3\sigma_0^2, \qquad (16)$$

where

$$\beta_3 = c+\frac{c^2}{2}. \qquad (17)$$

The surface energies of the fibre and the matrix, γ_f and γ_m, respectively, are related to the potential energy difference as

$$2\gamma_f S_f = \Delta U_f(\, c_1+\frac{c_2}{2}\ \ (2\theta) \qquad (18)$$

and

$$2\gamma_m S_m = \Delta U_m\ \ c_1+\frac{c_2}{2}\ \ (2\pi-2\theta), \qquad (19)$$

where S_f is the sectional area of the fibres, $S_f = 2S$, and S_m is the sectional area of the matrix, $S_m = \pi\{(c_1+c_2)^2 - c_1^2\} - S_f$. The sum of S_f and S_m is the area swept by the penny-shaped crack during the crack penetration. Finally, using Equations 2, 14, 16, 18, and 19, we obtain the applied stress, σ_{02}, for the penny-shaped crack penetrating the fibres completely as

$$\sigma_{02} = \left(\frac{(2\gamma_f S_f + 2\gamma_m S_m) E_m}{\pi(2c_1 + c_2)\{(1-\nu_f^2)\beta_2\theta + (1-\nu_m^2)\beta_3(\pi-\theta)\}c_1^2} \right)^{1/2}. \quad (20)$$

2.2. Debonding of the interface

In this section, the case where a penny-shaped crack propagates along the cylindrical interface between the fibres and matrix, i.e., the debonding of the interface, is considered. The theoretical model assumes that after having touched two neighbouring fibres, the penny-shaped crack expands concentrically without cutting these fibres, as shown in Fig. 6a, and then, the crack propagates along the interface of fibres, as shown in Fig. 6b. Also, in this section are derived the applied stresses, σ_0, required for the initiation of debonding crack (σ_{03}) and for the complete debonding of the interface (σ_{04}) over the total length of fibre.

2.2.1. Initiation of debonding crack

We consider a cylindrical region with radius of $c_1 + c_2$ and height, l, including two fibres as shown in Fig. 6b. The strain in the debonded fibre region is denoted by ϵ_2 in Fig. 6b. Elsewhere, the strain is assumed to have the uniform value of ϵ_1. A consideration of static equilibrium leads to

$$\epsilon_1 = \frac{(c_1 + c_2)^2 \sigma_0}{E_m\left\{(c_1 + c_2)^2 - \frac{c_2^2}{2}\right\} + E_f \frac{c_2^2}{2}} \quad (21)$$

and

$$\epsilon_2 = \frac{2(c_1 + c_2)^2 \sigma_0}{E_f c_2^2}, \quad (22)$$

where σ_0 is the average applied stress over the fibre and matrix areas.

Next, the total potential energy change due to the initiation of the debonding crack is considered. The total energy change is obtained from the changes in the surface energy and strain energy, as well as from the work done by the applied force. The surface energy change can be obtained as

$$dU_1 = 4\pi c_2 \Delta x R_{Di}, \quad (23)$$

where Δx is the infinitesimal length of the debonded region and R_{Di} is the interface fracture energy. R_{Di} can also be considered as the strain energy release rate for the initiation of debonding, because the fracture energy is supplied by the release of the strain energy upon crack initiation. It is assumed that there is no change of strain in the matrix region of height $2\Delta x$ while the strain in the fibre region of height $2\Delta x$, changes from ϵ_1 to ϵ_2. Then, the strain energy change in the fibre region denoted by Δx is

$$dU_2 = \tfrac{1}{2} E_f(\epsilon_2^2 - \epsilon_1^2)\pi c_2^2 \Delta x. \quad (24)$$

The work done by the applied force is

$$dU_3 = 2\sigma_0 \pi (c_1 + c_2)^2 (\epsilon_2 - \epsilon_1)\Delta x. \quad (25)$$

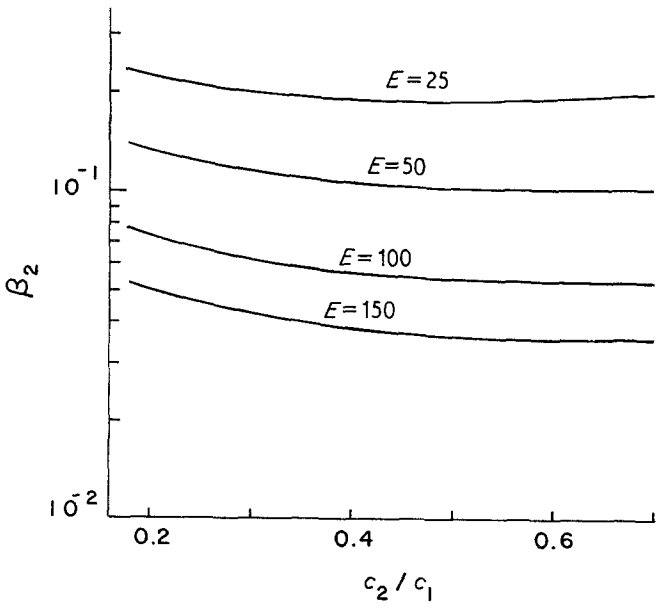

Figure 5 Non-dimensional parameter, $\beta_2 = \Delta U_f/\pi(1-\nu_m^2)c_1^2\sigma_{02}^2/E_m$, related to the fracture energy for the crack completely penetrating into the fibres.

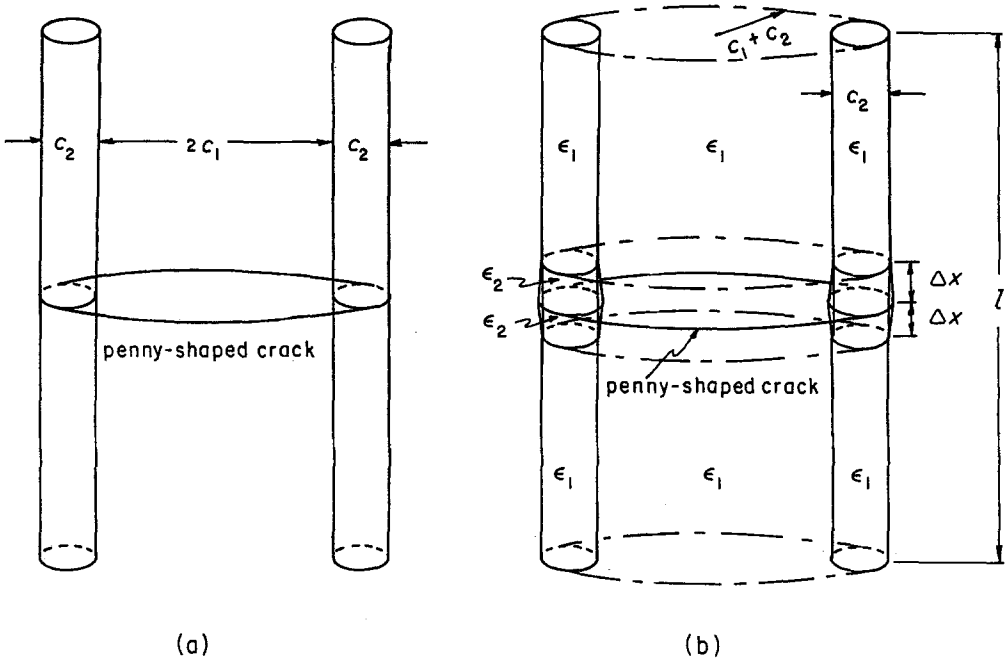

Figure 6 (a) The concentric propagation of a penny-shaped crack without cutting fibres; (b) The initiation of debonding of matrix–fibre interface by a penny-shaped crack propagated concentrically without cutting the fibres.

Since the net energy change is zero,

$$dU_1 + dU_2 - dU_3 = 0. \tag{26}$$

A substitution of Equations 21 to 25 into Equation 26 yields

$$R_{Di} = \frac{\sigma_0^2 c_1}{E_m} \beta_4, \tag{27}$$

where

$$\beta_4 = \frac{\left\{(1+c)^2 - \frac{c^2}{2}\right\}^2 (1+c)^4}{2c^3\left\{(1+c)^2 + (E-1)\frac{c^2}{2}\right\}^2 E} \tag{28}$$

and β_4 is the non-dimensional strain energy release rate for the initiation of the debonding crack. β_4 is plotted as a function of c_2/c_1 in Fig. 7 for several values of E.

The strain energy release rate, R_i, is related to the interface fracture energy γ_I as

$$R_{Di} = \gamma_I. \tag{29}$$

Then, using Equations 27 to 29, the applied stress ($\sigma_0 \equiv \sigma_{03}$) required for the initiation of the debonding crack can be easily obtained

$$\sigma_{03} = \left(\frac{\gamma_I E_m}{c_1} \frac{1}{\beta_4}\right)^{1/2}. \tag{30}$$

2.2.2. Propagation of debonding crack

The propagation of the debonding crack along the interface is depicted in Fig. 8. Unlike the case of the initiation of the debonding crack, there is a change of strain in the matrix region of thickness Δx when the crack propagates a distance Δx. Since the matrix strain in the debonded region (AACC and BBCC in Fig. 8) vanishes, the strain change is from ϵ_1 to zero. Then, the strain energy change in the matrix region of thickness Δx is

$$dU_2' = -E_m \epsilon_1^2 \pi \left\{(c_1 + c_2)^2 - \frac{c_2^2}{2}\right\} \Delta x. \tag{31}$$

The other energy changes are the same as those described in the case of initiation.

Substituting Equations 23 to 25 and 31 into Equation 26, we obtain the strain energy release rate, R_{Dp}, for the propagation of debonding as

$$R_{Dp} = \frac{\sigma_0^2 c_1}{E_m} \beta_5, \tag{32}$$

where

$$\beta_5 = \frac{\left\{(1+c)^2 - \frac{c^2}{2}\right\}(1+c)^4}{2c^3\left\{(1+c)^2 + (E-1)\frac{c^2}{2}\right\} E} \tag{33}$$

and β_5 is the non-dimensional strain energy release

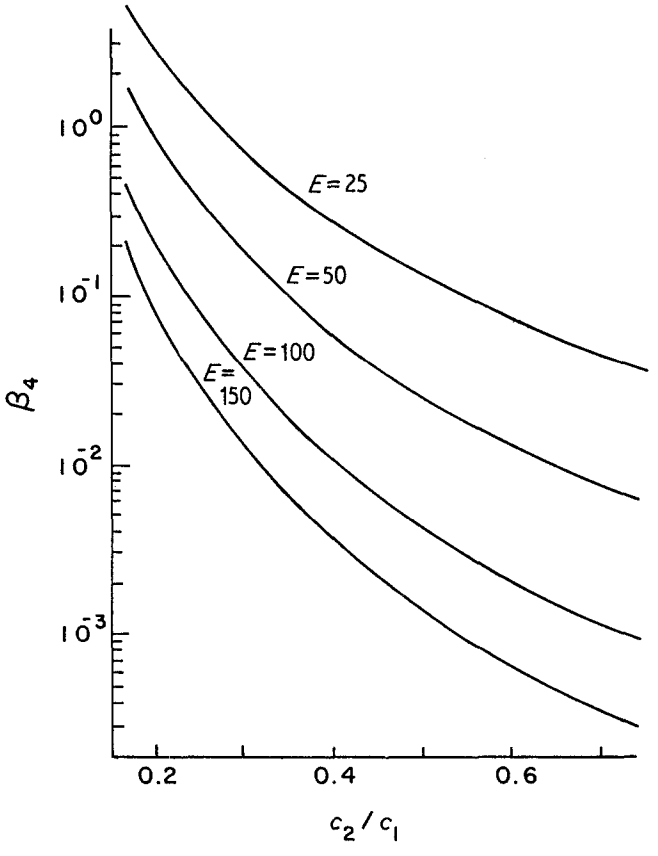

Figure 7 Non-dimensional strain energy release rate, $\beta_4 = R_{\mathrm{Di}}/c_1\sigma_{03}^2/E_{\mathrm{m}}$, for the initiation of a debonding crack.

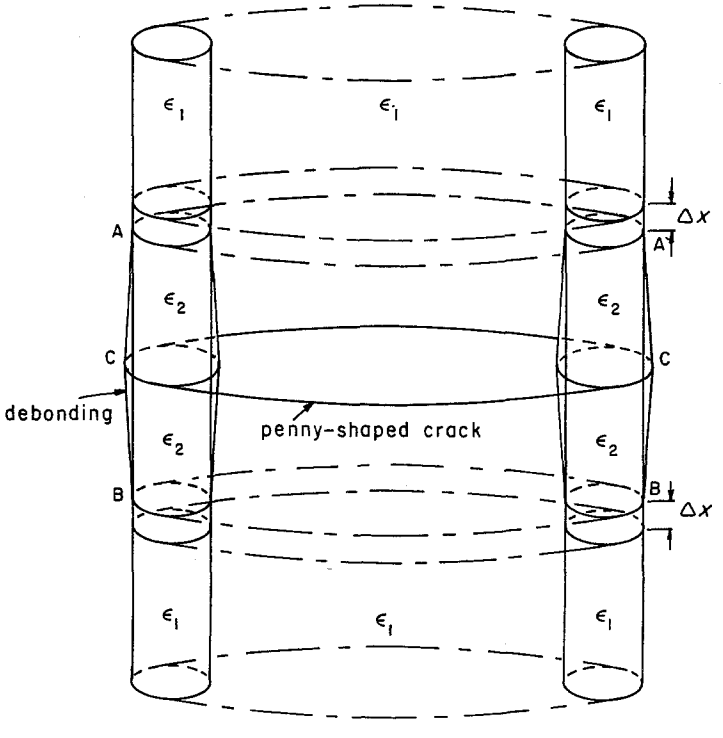

Figure 8 The propagation of the debonding crack along the matrix–fibre interface.

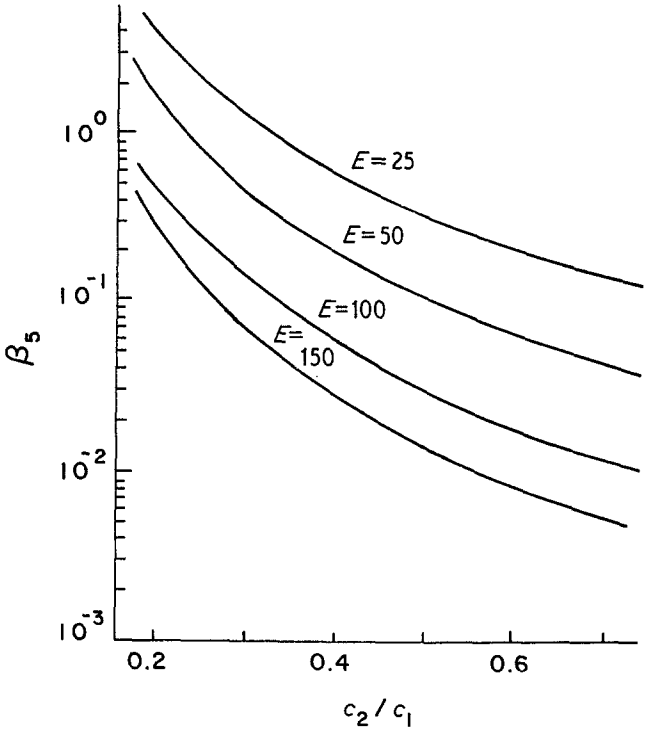

Figure 9 Non-dimensional strain energy release rate, $\beta_5 = R_{Dp}/c_1\sigma_{04}^2/E_m$, for the propagation of debonding crack along the matrix–fibre interface.

rate. β_5 is plotted as a function of c_2/c_1, in Fig. 9 for several values of E.

It is assumed that the strain energy release rate, R_{Dp}, remains constant during the propagation of the debonding crack to the fibre end. Then, the total strain energy change from the initiation of the debonding crack to the complete debonding of the fibre lateral surface is given by

$$\Delta U_D = 2R_{Dp}l\pi c_2. \quad (34)$$

Therefore, the difference in the total potential energy between the initial stage that a penny-shaped crack just meets the fibres and the final stage that the debonding crack propagates to the fibre end becomes $\Delta U_D + \Delta U'_m$. Here, $\Delta U'_m$ is the change in the total potential energy from the time when the penny-shaped crack just meets the neighbouring fibres to that when the crack expands to surround the fibres, as shown in Fig. 6a. Using the same model as used in Section 2.1.2, $\Delta U'_m$ is found to be $\Delta U_m(2c_1 + c_2)(\pi - \theta)$. Also, ΔU_D is related to the interfacial fracture energy γ_I such that

$$\Delta U_D = 2l\pi c_2\gamma_I. \quad (35)$$

Then, from Equations 19 and 35,

$$\Delta U_D + \Delta U'_m = 2l\pi c_2\gamma_I + 2\gamma_m S_m. \quad (36)$$

Finally, the applied stress σ_{04} required for the penny-shaped crack debonding the whole lateral surface of the fibre is obtained from Equations 16, 32 and 34 to 36, such that

$$\sigma_{04} = \left(\frac{(2l\pi c_2\gamma_I + 2\gamma_m S_m)E_m}{2c_1 l\pi c_2\beta_5 + \pi(1-\nu_m^2)c_1^2(2c_1 + c_2)(\pi - \theta)\beta_3}\right)^{1/2}. \quad (37)$$

3. Results and discussion

3.1. Comparison with the result of an ideal composite

Sanchez-Moya and Pipkin [7] computed the strain energy release rate for a two-dimensional crack meeting the interface at a right-angle. The model used by Sanchez-Moya and Pipkin is called the "ideal composite model" and is based on the assumption that the fibre diameter, c_2, is infinitesimal and the fibre stiffness is infinite. Hence, the result of an ideal composite, which is plotted as a filled circle in Fig. 4, should correspond to the asymptotic value as c_2/c_1 and $E(= E_f/E_m)$

approach to 0 and ∞, respectively. Indeed, this is so as seen from Fig. 4.

3.2. Computation of σ_{01}, σ_{02}, σ_{03} and σ_{04}

In order to estimate the critical applied stresses necessary for the breakage of fibres and the debonding of the interface by a penny-shaped crack, the following material properties of a graphite fibre-reinforced composite are used: for the epoxy, $E_m = 3.5 \times 10^9\ N m^{-2}$, $\nu_m = 0.4$ and $\gamma_m = 330\ J m^{-2}$; for the graphite fibre, $E_f = 2 \times 10^{11}\ N m^{-2}$, $\nu_f = 0.17$ and $\gamma_f = 75\ J m^{-2}$ [13]. It is also assumed that $c_2 = 0.007$ mm and $l = 0.35$ mm. By adopting the fibre volume-fraction of $V_f = 0.2$, $c_2/c_1 = c = 0.289$. In order to estimate the applied stress, it is necessary to know the data of the interfacial fracture energy, γ_I. Murphy and Outwater [8] and Kelly [9] performed fibre pull-out tests for measuring γ_I. Using the above data, γ_I is calculated, based upon their model and it is found that $\gamma_I = 3.73\ J m^{-2}$. The fibre fracture strength of $\sigma_f = 1.6 \times 10^9\ N m^{-2}$ [13] has been used in this calculation. Kendall [14], also, carried out peel tests for obtaining data of the interface fracture energy. His value for the interface between polyethylene and silica is about $1\ J m^{-2}$, and is comparable to our calculated value, which will be used to estimate the applied stresses σ_{03} and σ_{04} for debonding of the interface (Case 1).

However, the method of measurements of γ_I has not been well established. Moreover, the value of γ_I is generally sensitive to the fibre surface treatment. Therefore, simply as a demonstration of the effect of γ_I on the debonding criteria, we also use the value $\gamma_I = 250\ J m^{-2}$ (Case 2). This value is of the same order as the values tabulated in [9] for other composite materials.

First, by the use of the γ_I value in Case 1, the above data of material properties, and Equations 6, 20, 30 and 37, the applied stresses, σ_{01}, σ_{02}, σ_{03} and σ_{04} are calculated as follows:

$$\sigma_{01} = 163\ MN m^{-2};$$
$$\sigma_{02} = 177\ MN m^{-2};$$
$$\sigma_{03} = 57\ MN m^{-2}; \text{ and}$$
$$\sigma_{04} = 110\ MN m^{-2}.$$

As far as stresses are concerned, the failure mode most likely to occur is the one which requires the lower applied stress. According to the above results, in both cases of initiation ($\sigma_{01} > \sigma_{03}$) and propagation ($\sigma_{02} > \sigma_{04}$), interface debonding is the dominant failure mode.

Next, in Case 2 of γ_I, the applied stresses for the initiation and propagation of the debonding are estimated, respectively, as follows:

$$\sigma_{03} = 475\ MN m^{-2}; \text{ and}$$
$$\sigma_{04} = 263\ MN m^{-2}.$$

Comparing these values with the results of σ_{01} and σ_{02} in Case 1, we conclude that penetration is more likely to occur than debonding. These results have demonstrated that the failure mode is sensitive to the value of γ_I.

4. Conclusions

A theoretical study of the failure mode of a penny-shaped crack meeting adjacent fibres at a right-angle in a short-fibre reinforced composite has been attempted. The results in the present study have led us to the following conclusions:

(a) For given material data of a short graphite fibre composite, the debonding of the interface is dominant failure mode when the value of γ_I is small. For the larger value of γ_I, however, the penetration of the meeting crack is more likely to occur. Thus the failure mode is highly sensitive to the interfacial fracture energy, γ_I.

(b) The Kendall model, after it is extended to a three-dimensional case, has proved to be a very powerful method in the fracture analysis of composites.

(c) The experimental method to measure the interfacial fracture energy, γ_I, must be well established.

References

1. P. T. CURTIS, M. G. BADER and J. E. BAILEY, *J. Mater. Sci.* **13** (1978) 379.
2. T. W. CHOU and A. KELLY, *Ann. Rev. Mater. Sci.* **10** (1980) 229.
3. M. TAYA and T. MURA, *J. Appl. Mech.* **48** (1981) 361.
4. Y. TAKAO, M. TAYA and T. W. CHOU, *J. Appl. Mech.*, to be published.
5. D. B. BOGY, *J. Appl. Mech.* **38** (1971) 911.
6. M. COMNINOU, *ibid.* **46** (1979) 97.
7. V. SANCHEZ-MOYA and A. C. PIPKIN, *Int. J. Solids Structures* **13** (1977) 571.
8. M. C. MURPHY and J. O. OUTWATER, Proceedings of the 28th Annual Technical Conference, Reinforced Plastics/Composites Institute, Washington, D.C., February 1973 (The Society of the Plastic Industry, Inc, 1973) p. 17-A.

9. A. KELLY, *Proc. Roy. Soc.* **A319** (1970) 95.
10. R. S. WILLIAMS and K. L. REIFSNIDER, "Fracture Mechanics" ASTM STP677(1979) 629.
11. K. KENDALL, *Proc. Roy. Soc.* **A341** (1975) 409.
12. *Idem, ibid.* **A344** (1973) 287.
13. D. C. PHILLIPS and A. S. TETELMAN, *Composites* **3** (1972) 216.
14. K. KENDALL, *Brit. Polymer J.* **10** (1978) 35.

Received 10 June
and accepted 28 July 1981